Oncogene (2006) 25, 1571–1583

www.nature.com/onc

ONCOGENOMICS

Identification of novel genomic markers related to progression to glioblastoma through genomic profiling of 25 primary glioma cell lines

G Roversi[1], R Pfundt[2], RF Moroni[1], I Magnani[1], S van Reijmersdal[2], B Pollo[3], H Straatman[4], L Larizza[1] and EFPM Schoenmakers[2]

[1]Department of Biology and Genetics, University of Milan, Milan, Italy; [2]Department of Human Genetics, Radboud University Nijmegen Medical Centre, Nijmegen, The Netherlands; [3]Istituto Neurologico Besta, Milan, Italy and [4]Department of Epidemiology and Biostatistics, Radboud University Nijmegen Medical Centre, Nijmegen, The Netherlands

Identification of genetic copy number changes in glial tumors is of importance in the context of improved/refined diagnostic, prognostic procedures and therapeutic decision-making. In order to detect recurrent genomic copy number changes that might play a role in glioma pathogenesis and/or progression, we characterized 25 primary glioma cell lines including 15 non glioblastoma (non GBM) (I–III WHO grade) and 10 GBM (IV WHO grade), by array comparative genomic hybridization, using a DNA microarray comprising approx. 3500 BACs covering the entire genome with a 1 Mb resolution and additional 800 BACs covering chromosome 19 at tiling path resolution. Combined evaluation by single clone and whole chromosome analysis plus 'moving average (MA) approach' enabled us to confirm most of the genetic abnormalities previously identified to be associated with glioma progression, including +1q32, +7, −10, −22q, *PTEN* and *p16* loss, and to disclose new small genomic regions, some correlating with grade malignancy. Grade I–III gliomas exclusively showed losses at 3p26 (53%), 4q13–21 (33%) and 7p15–p21 (26%), whereas only GBMs exhibited 4p16.1 losses (40%). Other recurrent imbalances, such as losses at 4p15, 5q22–q23, 6p23–25, 12p13 and gains at 11p11–q13, were shared by different glioma grades. Three intervals with peak of loss could be further refined for chromosome 10 by our MA approach. Data analysis of full-coverage chromosome 19 highlighted two main regions of copy number gain, never described before in gliomas, at 19p13.11 and 19q13.13–13.2. The well-known 19q13.3 loss of heterozygosity area in gliomas was not frequently affected in our cell lines. Genomic hotspot detection facilitated the identification of small intervals resulting in positional candidate genes such as *PRDM2* (1p36.21), *LRP1B* (2q22.3), *ADARB2* (10p15.3), *BCCIP* (10q26.2) and *ING1* (13q34) for losses and *ECT2* (3q26.3), *MDK, DDB2*, *IG20* (11p11.2) for gains. These data increase our current knowledge about cryptic genetic changes in gliomas and may facilitate the further identification of novel genetic elements, which may provide us with molecular tools for the improved diagnostics and therapeutic decision-making in these tumors.

Oncogene (2006) **25,** 1571–1583. doi:10.1038/sj.onc.1209177; published online 24 October 2005

Keywords: glioma; array-based CGH; copy number changes; chromosome 19

Introduction

Gliomas are the most frequently occurring primary brain tumors in humans, and can be subdivided into three histological subtypes, that is, astrocytoma, oligodendroglioma and mixed oligoastrocytoma (OA), each characterized by a different grade of malignancy according to the WHO classification (Kleihues and Cavenee, 2000). Despite recent technical improvements in radiological and pathological diagnostic procedures, as well as the increasing knowledge on glioma biology and genetics, the possibilities for effective treatment and prognosis remain poor, especially for patients affected by glioblastoma (GBM) (the most aggressive astrocytic form), who have an average survival of <1 year after diagnosis (Simpson *et al*., 1993). At the other side of the prognostic spectrum, oligodendroglial tumors exhibiting loss of chromosomal arms 1p and/or 19q show a better response to chemotherapy and, consequently, a better prognosis (Cairncross *et al*., 1998; Ino *et al*., 2001; Jeuken *et al*., 2004).

Difficulties in clinical management (e.g. treatment and prognosis) are related to the complex identity of gliomas, which impairs a clearcut classification needed for discrimination between different tumor subtypes. Limitations of the actual diagnostic criteria are pointed out by data on both the different combinations of genetic lesions in tumors sharing similar histology, grade and intratumor genetic heterogeneity (Noble and Dietrich, 2004). For these reasons, there is a growing awareness that genome-wide and high-resolution genetic analyses will contribute to the improvement of the

Correspondence: Professor L Larizza, Department of Biology and Genetics for Medical Sciences, University of Milan, Via Viotti 3/5, Milano 20133, Italy.
E-mail: lidia.larizza@unimi.it
Received 7 April 2005; revised 9 August 2005; accepted 9 September 2005; published online 24 October 2005

current WHO classification by constructing a more objective molecular taxonomy of gliomas (Mischel *et al*., 2004).

For this purpose, over the last decade molecular approaches including mutation screening, comparative genomic hybridization (CGH) and loss of heterozygosity (LOH) analyses have led to the identification of the most frequently recurring genomic imbalances correlating to each WHO subtype (Koschny *et al*., 2002; Shapiro, 2002; Kitange *et al*., 2003) and to the identification of several genes acting in pathways involved in glioma development, either in the initiation stages (*p53* and *Ras* by *PDGF-NF1*) or in malignant progression (*Rb-CDKN2-CDK4*) (Zhu and Parada, 2002; Collins, 2004). Deletion of 19q is of particular interest, as it is shared by all three glioma subtypes, occurring in approximately 75% of oligodendroglioma, 45% of mixed OA and 40% of astrocytoma (von Deimling *et al*., 1992, 1994), where it is associated with the transition from low-grade to anaplasic tumors (Ohgaki *et al*., 1995; Ritland *et al*., 1995; Smith *et al*., 1999). Furthermore, similarly to oligodendroglioma, combined LOH of 1p and 19q was found to define a small subset of GBM patients with a significantly better survival, even if their tumors are not morphologically distinguishable from the bulk of GBMs (Schmidt *et al*., 2002).

A candidate tumor suppressor region has been assigned by LOH studies to 19q13.3, but no prime positional functional candidate gene in this band has yet been identified (Hartmann *et al*., 2002). We postulated a possible role for the novel serine threonine kinase gene *MARK4*, which maps at the centromeric boundary of the 19q13.3 LOH region, and which is overexpressed and duplicated in three GBM cell lines (Beghini *et al*., 2003).

In order to improve our current knowledge on both gross and subtle genetic changes involved in glioma initiation and progression, we interrogated 25 primary cell lines at the whole genome level by array-based comparative genomic hybridization (array-CGH or aCGH) at a 1 Mb resolution. Since chromosome 19 is of particular interest in the context of clinical decision-making, a full genomic chromosome 19 tiling path was also present on our arrays (our current resolution on chromosome 19 is in theory around 50 kb, and in practice around 100 kb).

Few high-resolution aCHG studies on gliomas are currently available to complement previously published CGH, SKY and LOH analyses (Cowell *et al*., 2004a, b; Bredel *et al*., 2005; Kitange *et al*., 2005; Nigro *et al*., 2005), which have all demonstrated an excellent correlation between the findings obtained through this approach, and those obtained by alternative techniques, stressing the usefulness and overall accuracy of this genomic approach as compared to classic most widely employed analyses (Cowell *et al*., 2004a, b).

Comparative analysis of elaborated aCGH data obtained on our cell lines collection allowed us to identify copy number changes shared by various glioma grades as well as aberrations apparently related to progression to GBM. Besides the confirmatory copy number alterations previously identified in gliomas, we also identified several genomic intervals containing novel candidate genes involved in gliomagenesis and/or progression recurrently found to be affected. Further clinical validation of these intervals by dedicated approaches might enable their inclusion among the genetic markers useful for a prognostic classification of gliomas, and is expected to ultimately lead to improved clinical decision-making.

Results

Recurrent genomic imbalances

Aiming at the detection of recurrent genomic copy number changes involved in glioma genesis and/or progression, we characterized 15 grade I–III gliomas (defined as 'non-GBMs') and 10 GBMs primary cell lines (Supplementary Table A) by aCGH on a 3.5k whole genome plus full-coverage chromosome 19 BAC array. Figure 1 depicts all the autosome ideograms (except chromosome 19, which is shown separately and in more detail in Figure 3) with the corresponding copy number changes identified in each cell line by the combined application of two statistical approaches: the whole chromosome association analysis and the 'moving average (MA)' algorithm. Whole chromosome association analysis defines entirely gained or lost chromosomes (Hackett *et al*., 2003), whereas the 'MA algorithm' allowed us to cluster gained or lost clones with aberrant average ratios in consecutive areas of copy number changes (Schraders *et al*., 2005). For more defined regions affecting at least four cases of partial chromosomal arm imbalance, the smallest regions of overlap (SROs), defined as the minimal regions of deletion/gain overlap, were also determined as shown in Table 1, where detailed clone information as well as the physical location (Mb positions) of the encompassing and flanking clones is also provided.

Figure 1 and Table 1 show genomic imbalance affecting either specifically GBMs or non-GBMs or, alternatively, both. The most frequent changes exclusive for GBMs involve complete or partial gain of chromosome 7 (70%), loss of chromosomes 10 (100%) and 22 (40%) (Kitange *et al*., 2003), which are known to be involved in glioma progression, as well as gain at 1q32 (Riemenschneider *et al*., 2003), detected in three GBMs and in one non-GBM. We also identified novel recurrent findings unreported in previous studies. We found that only GBMs show loss of chromosome 18 (40%) and gain of the entire chromosome 21 (50%). Double I-FISH using two chromosome 21 BACs lying $\sim$7 Mb apart from each other confirmed the aCGH gain in showing a very high number (>8) of signals for both probes in the great majority of nuclei of the representative MI-7 cell line (chromosome 21 average $\log_2$ ratio $= +0.3$) (see Supplementary Figure A).

A small overlapping region mapping at 4p16.1 is also specifically lost in four (40%) GBM cell lines.

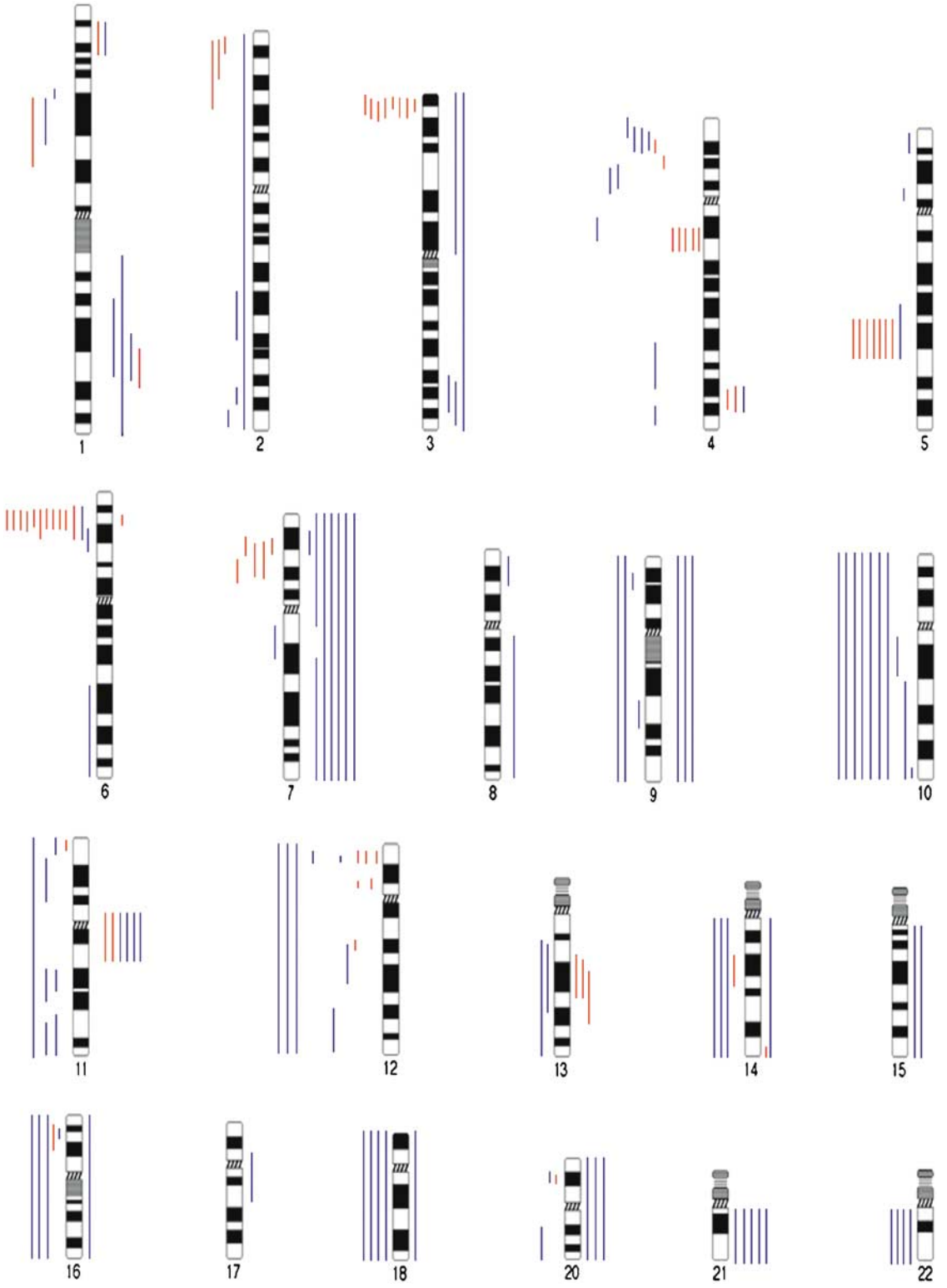

Figure 1 Copy number changes as identified by statistical analysis of the aCGH data. All chromosome ideograms are depicted, with the exceptions of sex chromosomes (not included in the analysis), and chromosome 19, which is shown at increased resolution in Figure 3. Bars of different color for 'non-GBMs' (red) and GBMs (blue) are placed on the right and on the left of each chromosome ideogram to indicate both gains and losses, respectively.

Table 1 Smallest regions of overlapping imbalances (SROs) shared by at least four cases of partial chromosomal arm gain/loss

Chr.	*Gain/loss*	*Upper flanking clone*	*Lower flanking clone*	*Physical interval (Mb)*	*Cytogenetic interval*	*Incidence 10 GBMs 15 non-GBMs*
1q	Gain	RP11-148K15	RP11-145I13	201.30–203.75	1q32.1	1 non-GBM 3 GBMs
3p	Loss	RP11-121D3	RP11-32F23	2.21–4.19	3p26.1–p26.3	8 non-GBMs
4p	Loss	Rp11-97H19	RP11-34C20	6.87–11.01	4p16.1	4 GBMs
4p	Loss	RP11-89H17	RP11-151G21	17.28–20.12	4p15.31–p15.32	1 non-GBMs 3 GBMs
4q	Loss	RP11-234L24	RP11-105F22	67.57–77.45	4q13.2–q21.1	5 non-GBMs
5q	Loss	RP11-64F17	RP11-45L19	112.71–128.33	5q22.2–q23.3	7 non-GBMs 1 GBM
6p	Loss	RP11-53P21	RP11-83B17	1.41–14.55	6p23–p25.3	11 non-GBMs 1 GBMs
7p	Loss	RP11-123E5	RP11-243C6	17.33–22.68	7p15.3–p21.1	4 non-GBMs
11	Gain	RP11-29O22	RP11-20K4	46.58–67.22	11p11.2–q13.2	3 non-GBMs 3 GBMs
12p	Loss	RP11-96B19	RP11-72J9	11.74–14.23	12p13.1–p13.2	3 non-GBMs 5 GBMs

Mb position and chromosome bands of the clones are as listed by the UCSC genome browser (May 2004 freeze).

Three SROs mapping at 3p26, 4q13–21 and 7p15–21 turn out to be exclusively lost in, respectively, eight (53%), five (33%) and four (26%) of non-GBMs, whereas both glioma groups share partial losses at 4p15, 5q, 6p and 12 p and gains at 11p–q (Table 1).

In addition, the use of the 'MA' algorithm allowed us to estimate which areas are quantitatively more involved within entirely gained or lost chromosomes such as chromosomes 10 and 7, the two most frequent aberrations found in gliomas. As depicted in Figure 1, seven GBM cell lines showed loss of the entire chromosome 10. As shown in Figure 2, three distinct areas emerged in all cell lines by using this algorithm. The three areas on chromosome 10 encompass several candidate tumor suppressor genes, including *KLF6*, *LGI1*, *PTEN*, *DMBT1*, *WDR11* and *MXI1*, already known to be indeed associated with glioma progression (Chernova *et al*., 2001; Manni *et al*., 2002; Kohler *et al*., 2004). One region spans from 10pter to 10p14, with a peak between clones RP11-89B19 and RP11-80D10 at 10p15.3 telomerically to *KLF6*; only the *ADARB2* gene, a brain-specific adenosine deaminase, resides within this interval. The second interval, mapping at 10q22.2–10q23.33, shows a peak of loss at 10q22.3, centromerically to *PTEN* between clones RP11-45P20 and RP11-342M3 and includes five annotated genes. The third region, spanning 10q25–26, has a peak at 10q26.13–q26.2 between clones RP11-70E19 and RP11-32H11 and telomeric to *DMBT1*: the peak loss area comprises 12 fully assigned genes.

When chromosome 7 was tested by the same approach, a homogeneous trend of imbalance along the entire chromosome was revealed, and no recurrent areas with significant deviation from whole chromosome average could be detected (data not shown).

DNA copy number changes detected by the full chromosome 19 coverage subarray

Motivated by the frequent involvement of chromosome 19q in gliomas (von Deimling *et al*., 1992, 1994; Ohgaki *et al*., 1995; Ritland *et al*., 1995; Smith *et al*., 1999; Schmidt *et al*., 2002) and our recent data on the duplication of *MARK4* in three GBM cell lines (Beghini *et al*., 2003), we pursued a high-resolution characterization of chromosome 19 in our cell lines through the use of full genomic coverage aCGH for this particular chromosome.

By applying the 'MA' algorithm, two frequently gained regions of interest, mapping to 19p13.11 and 19q13.13–13.2, respectively, emerged, for each of which a SRO could be defined (Figure 3).

The 19p13.11 interval, with a SRO spanning about 350 kb (from RP11-365K12 to RP11-350I20) encompasses 13 genes and was gained in three non-GBM and four GBM cell lines. The 19q13.13–13.2 interval was gained in three non-GBM and four GBM cell lines too. This latter 630 kb interval (from RP11-1031M21 to RP11-452P05) contains 16 genes. Moreover, we were able to detect at 19p13.2 (8.55–8.81 Mb) a region of copy number changes (lost and gained) in 20 cell lines as well in three normal versus normal hybridizations. By further analysis, we could establish that copy number changes behaved in a 'hybridization reference-dependent' way (data not shown), confirming its polymorphic nature, consistent with the information on clone RP11-79F15 provided by the Genome Variation Database (http://projects.tcag.ca.variation) (Iafrate *et al*., 2004; Sebat *et al*., 2004). In our normal controls, the largest polymorphic region spans 260 kb, and is located between clones RP11-92E05 and RP11-203K06.

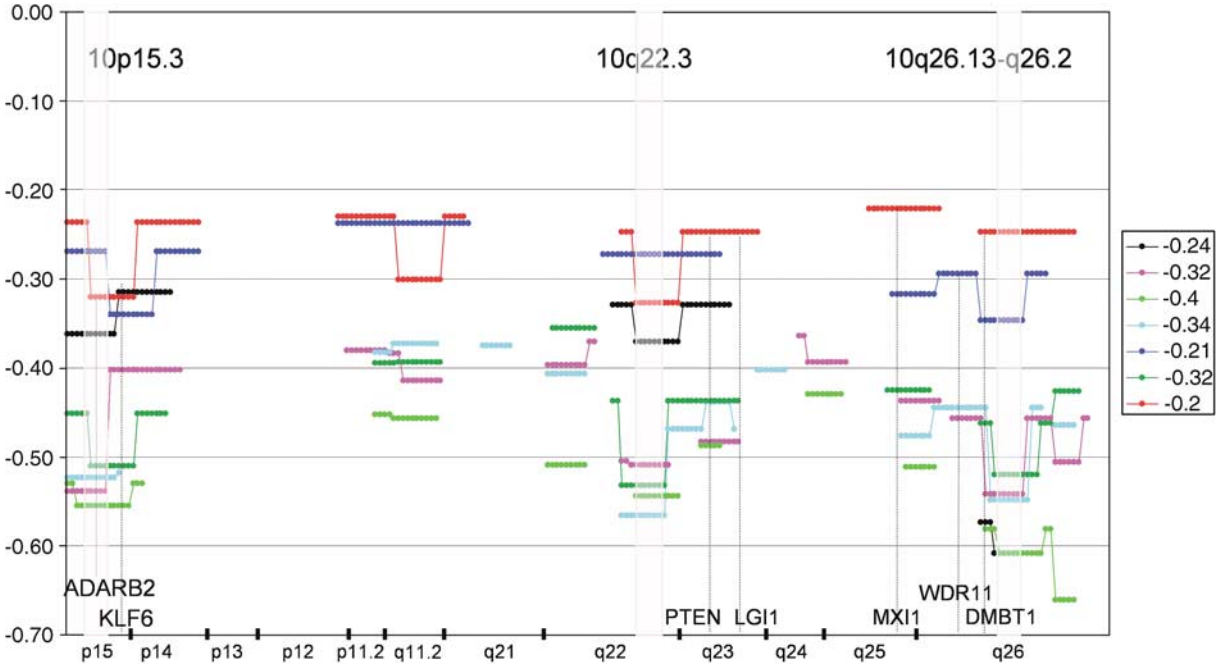

Figure 2 Most extreme moving average intervals on chromosome 10. Chromosomal bands and moving average values are depicted on the *X*- and *Y*-axis, respectively. Each cell line is marked by a different color and in the caption the corresponding whole chromosome average values are reported. Gray boxes indicate the peaks of the most extreme moving average. The map position of most fully annotated tumor suppressors and candidate tumor suppressors is indicated.

By means of the 'MA' algorithm, we also found that the interval characterized by five overlapping clones, and containing the entire *MARK4* gene, belongs to a region of gain in three non-GBM (MI-67, MI-26, G43) and one GBM (MI-4) cell lines. Moreover, a GBM cell line (MI-63) showed a gained region partially included in the *MARK4* overlapping clones, while only one non-GBM cell line (MI-13, AOA) presented a deletion in the candidate tumor suppressor region 19q13.3 stretching to *MARK4*. The SRO gained region, placed at the centromeric boundary of LOH tumor suppressor area (Figure 3), is comprised between clones RP11-752G09 and CTD-2344L03, where, besides *MARK4*, the creatine kinase, *CKM*, kinesin light chain, *KLC2*, the DNA repair genes, *ERCC1* and *2*, the inhibitor of *p53* function, *PPP1R13L*, and the nucleolar autoantigen gene, *ASE-1*, reside.

Single clone analysis

A total of 29 homozygously deleted clones ($\log_2$ ratio < -0.8) were identified in eight GBM cell lines (Table 2), whereas grade I–III glioma cell lines did not reveal any homozygously deleted clones. In all, 14 clones mapping to 12p12.1–p13.32 belong to a rather large ($\sim$23 Mb) area of deletion in the G32 cell line and a few reside in the previously described 12p SRO (Table 1). As the G32 cell line shows by aCGH the loss of the entire chromosome 12, in order to confirm that 12p13.1 (targeted by clone RP11–439G16, $\log_2$ ratio -0.85) is under-represented as compared to 12q (monitored by clone RP11–141F8, $\log_2$ ratio -0.25), we performed dual color I-FISH to evaluate the ratio between the number of signals given by the two clones. Scoring of 100 nuclei revealed that the ratio of 12q:12p copies as determined by aCGH (1.68:1.10 = 1.52) underestimated the ratio obtained by FISH (1.95) (see Supplementary Figure B). Only clone CTD-2154O24 mapping to chromosome 9p21 appeared to be deleted in more than one GBM cell line (MI-7 and MI-4) and contains the *CDKN2A* (*p16*) gene, a well-known tumor suppressor gene known to be involved in glioma progression (Zhu and Parada, 2002). Chromosomes 10 and 22 show multiple regions of homozygous deletions. More specifically, clone RP11-129G17, which resides at 10q23 and flanks the *PTEN* gene, which is known to be of functional relevance in gliomas (Zhu and Parada, 2002; Rong *et al*., 2005), is homozygously deleted. In addition, two clones mapping to 10q26.2, although not consecutive, probably delimit the same deletion in cell line MI-63, as two clones between them present $\log_2$ ratio < -0.5. The observation of discontinuous intervals may be explained by ambiguous mapping positions, subject to change upon release of future, revised genome-builds. Indeed, most nuclei (92/100) of the MI-63 cell line did not show any hybridization signal following I-FISH with the RP11-32H11 clone labeled either by green or red fluorescence (see Supplementary Figure C).

By comparing the frequencies of the most frequently heterozygously deleted clones ($\log_2$ ratio < -0.3) among 15 non-GBMs and 10 GBMs (Table 3), a picture

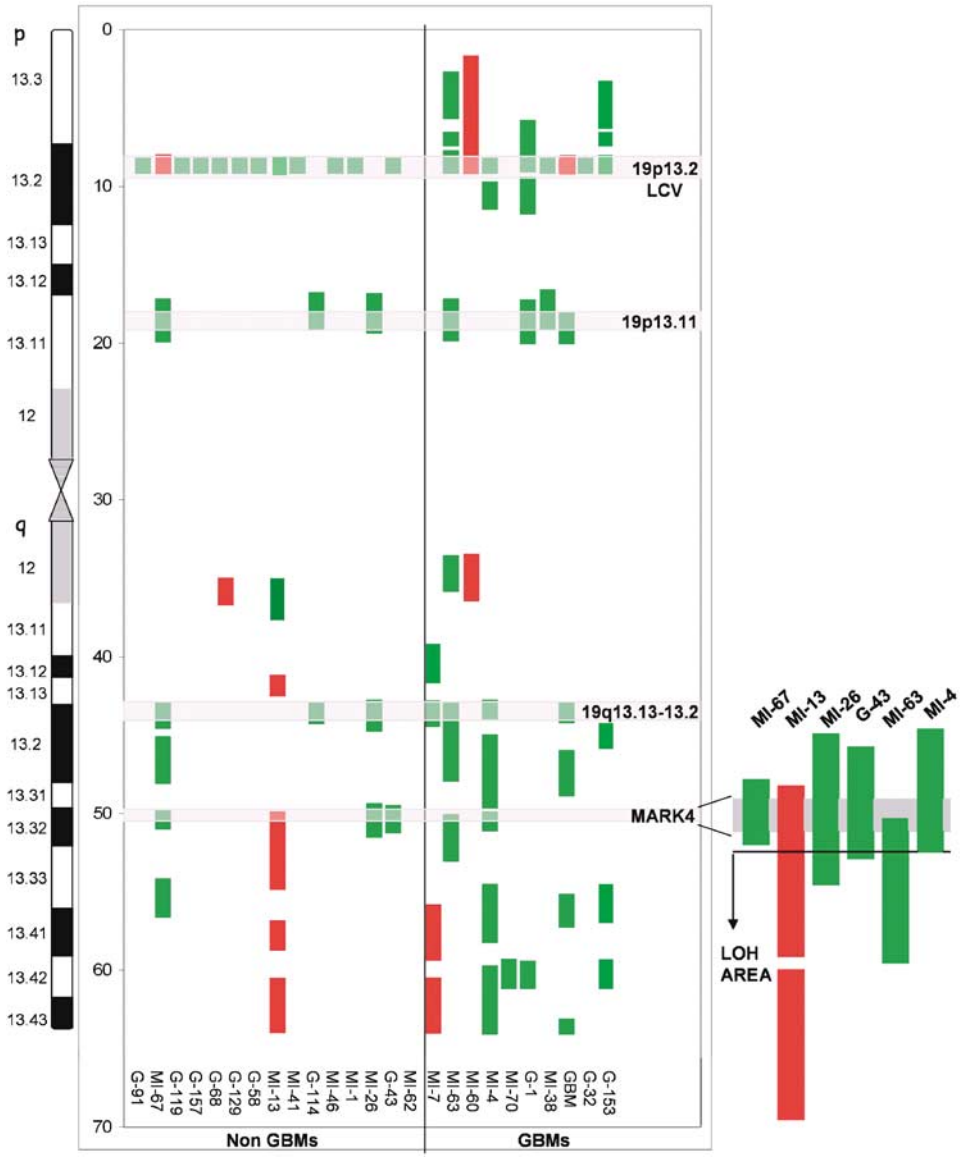

Figure 3 Chromosome 19 imbalance detected by full-coverage array. Each vertical line on the *X*-axis corresponds to a cell line. Mb position and chromosome bands are shown on the *Y*-axis. Losses are depicted in red, and gains in green. Gray lines indicate the SRO regions at 19p13.11, 19q13.13–13.2 and LCV at 19p13.2. *MARK4* clones at 19q13.3 are also indicated. Magnification of the region spanned by five overlapping clones (gray area) and entirely covering the *MARK4* gene is shown on the right.

emerges in which both glioma groups share high-frequency deletions for the clone RP11-709A23 at 12p11.23, whereas other clones are exclusively involved in one of the two histological subgroups. Among these, clones mapping to 3p26 and 4q13.3, which fall in the previously described SROs (a), stand out among non-GBMs, just as clones mapping at 12p13.1 (RP11-439G16 and RP11-1092P21), sorted also as homozygous deletions (c), emerge among GBMs.

We did not detect any clones with amplified signal intensities ($\log_2$ ratio >1), whereas gained clones showing a $\log_2$ ratio's between 0.5 and 1 (Table 4) were detected for 31 clones in I–III grade gliomas, and for 201 clones in GBMs. The majority maps to chromosome 7, belongs to cell lines with additional chromosome(s) 7 and is not involved in non-GBM cell lines, with the exception of RP5-953A4 at 7q11.23, which is gained in one non-GBM cell line too, and RP11-1143D24 at 19q12, which, to our knowledge, does not contain any annotated gene. Non-GBMs specific clones are nearly all listed as polymorphic clones in the Genome Variation Database (http://projects.tcag.ca.variation) (Iafrate *et al*., 2004; Sebat *et al*., 2004) and were all gained in GBM cell lines too. Gain signals with $\log_2$ ratio >0.3 (Table 5) were shared by both GBMs and non-GBMs for clone RP11-39G12, which, together with the polymorphic clone RP11–79A4, belongs to the 11p–q SRO previously identified by our MA approach (Table 1).

Table 2 Homozygous deleted clones (log_2 ratio <-0.8)

Clone name	*Chr. band*	*Mb position*	*Cell line*	*Annotated genes*
RP11-67J2	2q22.3	145.24	1 (G1)	*HNMT*, *NXPH2*, *LRP1B*, *KYNU*, *ARHGAP15*, *ZFHX1B*
RP11-14G17	6q16.2	99.73	1 (MI-7)	*FTU9*, *FHL5*, *GPR63*, *KIAA1900*, *POU3F2*, *FBXL4*, *COQ3*, *CCNC*, *PRDM13*
CTD-2097K16	9p21.3	21.95	2 (MI-7; MI-4)	***CDKN2A***
RP11-79C22	10p14	7.34	1 (MI-4)	***SFMBT2***, *ITIH5*, *ITIH2*, *KIN*, *ATP5C1*, *TAF3*
RP11-45P20[a]	10q22.3	78.69	1 (MI-4)	***KCNMA1+***
RP11-131C15	10q22.3	80.96	1 (MI-4)	***SFTPA2, SFTPA1, FAM22A, SFTPD, ANXA11***
RP11-129G17	10q23	90.17	1 (MI-60)	*PTEN*
RP11-32H11[a]	10q26.2	128.72	1 (MI-63)	*CTBP2*, *MMP21*, *UROS*, *BCCIP*, *DHX32,FANK1*, *ADAM12*, ***DOCK1***, ***PTPRE***, *MKI67*
RP11-48A2	10q26.2	129.80	1 (M-63)	
14 clones[a]	12p12.1–p13.32		1 (G32)	—
RP11-3P8	13q34	111.75	1 (MI-7)	*ING1*, *ANKRD10*, *ARHGEF7*, ***SOX1***, *TUBGCP3*
RP11-109J21	16q12.1	54.78	1 (T63)	*CES1*, ***GNAO1, AMFR***, *CPSF5*, *BBS2*, *Metallothioneins family1*, *SCL12A3*, *HERPUD1*, *CETP*, *CPNE2*, *ARL2BP*, *NIP30*, *TMASF11*
RP11-151M3	22q13.31	46.10	1 (MI-60)	*TAFA5*
RP11-354I12	22q13.32	47.48	1 (MI-60)	
RP11-179L12	22q13.33	47.82	1 (MI-60)	

Genes residing between the two flanking clones of losses are in italics, and with bolded characters for those mapping within clones. Chromosome 10 clones were not included in the frequency analysis because most of the GBM cell lines analysed lost the entire chromosome. [a]Clones falling in SRO (Table 1) and in peaks of loss in quantitative analysis of chromosome 10 (Figure 2).

Table 3 Most frequently heterozygous deleted clones (log_2 ratio <-0.3)

Clone name	*Chr. band*	*Mb position*	***% Non-GBMs***	*% GBMs*	*Annotated genes*
RP11–178M15	1p36.21	13.73	**35 (5/14)**	/	*T1A-2*, *PRDM2*
RP11–32F23[a]	3p26	4.16	**36 (4/11)**	/	*CNTN4*, *IL5RA*, *TRNT1+*, *LRRN1*
RP11–198G24[b]	3q26.1	165.27	**57 (8/14)**	/	*No genes*
RP11–108H14	4p14	36.99	6 (1/15)	**55 (5/9)**	*CENTD1*, *TBC1D1*, *PTTG2*
RP11–63E13	4q13.3	66.42	/	**66 (6/9)**	*AF307080*, *EPHA5*, *CENPC1*
RP11–117B11[a]	4q13.3	73.38	**38 (5/13)**	/	*GC*, *GPR74*, ***ADAMTS3***
RP11–88E14	6p22.3	16.49	**46 (6/13)**	/	*MYLIP*, *GMPR*, ***ATXN1***
RP11–163E21	6p22	16.76	**60 (6/10)**	33 (3/9)	***ATXN1***
RP11–15°11	11p14	23.93	**40 (6/15)**	20 (2/10)	*HTATIP2*, *HRMT1L3*, *SLC6A5*, *NELL1*, *TMEM16E*, *SLC17A6*, *FANCf*, *GAS2*, *MUC15*
RP11–439G16[a,c]	12p13.1	14	/	**60 (6/10)**	*RAI3*, *GPRC5D*, *HEBP1*, *GSG1*,
RP11–1092P21[a,c]	12p13.1	14.1	/	**70 (7/10)**	*EMP1*, ***GRIN2B***, *ATF7IP*,
RP11–72J9[a]	12p13.1	14.4	/	**66 (6/9)**	*GUCY2C*
RP11–92H16	12p12.1	21.7	7 (1/13)	**57 (4/7)**	***LDHB***, ***KCNJ8***, *ABCC9*
RP11–59N23	12p12.1	21.64	14 (2/14)	**55 (5/9)**	
RP11–709A23	12p11.23	27.7	**45 (5/11)**	**71 (5/7)**	***PPFIBP1***
RP11–12P7	14q22	52.12	7 (1/13)	**60 (6/10)**	*ERO1l*, *PSMC6*, *STYX*; *GNPNAT1*, *PLEKHC1*, *DDHD1*
RP11–814C11	19q13.31	49.81	**36 (4/11)**	/	*PVR+*

Genes residing between the two flanking clones of losses are in italics, and with bolded characters for those mapping within clones. Gray-shaded rows indicate clones of the chromosome 19 full-coverage array. Chromosome 10 clones were not included in the frequency analysis because most of the GBM cell lines analysed lost the entire chromosome. [a]Clones falling in SRO (Table 1) and in peaks of loss in quantitative analysis of chromosome 10 (Figure 2). [b]Clones/genes identified as polymorphic loci in the Genome Variation Database (http://projects.tcag.ca.variation). [c]Homozygously and high-frequency heterozygously deleted clones.

Table 4 Most frequently gained clones with $\log_2$ ratio >0.5

Clone name	*Chr. band*	*Mb position*	*GBMs*	*Genes*
RP11-172G5	3q26.3	174.54	3 of 10	*ECT2*, *SPATA16*, *NLGN1*
RP11-123E5	7p21	17.33	3 of 9	*TM4SF13*, *AHR*
RP11-87M15	7p14	36.47	3 of 10	***AOHA*** , *ELMO1*
RP5-953A4	7q11.23	74.59	4 of 9	*More than 15 genes plus* ***WBSCR20B***, ***PMS2L2***
RP11-49N15	7q21.3	92.53	3 of 10	*CALCR*
RP11-72J24	7q22.3	104.20	3 of 10	*PRES*, *RELN*, *ORC5L*, ***MLL5+***, *SYPL*, *PBEF1*, *PIK3CG*
RP11-148F17	7q33	136.66	3 of10	***DGK1***
RP11-43L19	7q36.2	150.93	3 of 10	*ABCF2*, *SMARCD3*, *NYREN18*, *RHEB*, *PRKAG2*, *GALNT5–11*, *MLL3*, *XRCC2*
RP1-3K23[a]	7qter	157	4 of 10	*PTPRN2*, *VIPR2*
RP11-93H24	13q14.3	52.11	3 of 10	***SUGT1LECT1***, ***LECT1***
RP11-1143D24	19q12	32.50	3 of 10	*No genes*
Clone name	*Chr. band*	*Mb position*	*Non-GBMs*	*Genes*
RP11-80L16[a]	6q12	67.14	4 of 14	*EGFL11*
RP11-79A4[a,b]	11p11.2	48.64	3 of 14	*PTPRJ*, *FOLH1*, *OR family*
RP11-598E05[a]	19p13.2	8.69	5 of 15	***OR2Z1***, ***MBD3L1***
RP11-1143D24	19q12	32.50	3 of 15	*No genes*

Genes residing between the two flanking clones of losses are in italics, and with bolded characters for those mapping within clones. Gray-shaded rows indicate clones of the chromosome 19 full-coverage array. [a]Clones falling in SRO (Table 1). [b]Clones/genes identified as polymorphic loci in the Genome variation Database (http://projects.tcag.ca.variation).

Table 5 Most frequently gained clones with $\log_2$ ratio >0.3

Clone name	*Chr. band*	*Mb position*	*% non-GBM*	*% GBM*	*Genes*
RP11-218I24	4q28.3	138.24	**40 (6/15)**	/	*PCDH18*, *SLC7A11*
RP11-80L16[a,b]	6q12	67.14	**64 (9/14)**	**60 (6/10)**	*EGFL11*
RP11-17O4	9q34.2	125.76	**40 (6/15)**	33 (3/9)	*More than 30 genes in the interval*
RP11-39G12[c]	11p11.2	46.58	**50 (6/12)**	**50 (5/10)**	*SYT13*, *CHST1*, *SLC35C1*, *CRY2*, *MAPK8IP1*, *PEX16*, *BHC80*, *CREB3L1*, *DGKZ*, *MDK*, *CHRM4*, ***ARHGAP1***, ***ZNF408***, ***F2***, ***ch-TOG***, *LRP4*, *MGC470*, *PACSIN3*, *DDB2*, *ACP2*, *NR1H3*, *IG20*, *MYBPC3*, *SPI1*, *PSMC3*
RP11-79A4[a,b,c]	11p11.2	48.64	**61 (8/13)**	33 (3/9)	*PTPRJ*, *FOLH1*, *OR family*
1129C9	19qter	64	**57 (8/14)**	33 (3/9)	***ZNF584***, ***ZNF132***, ***ZNF324***, ***SLC27A5***, ***ZNF499***, ***TRIM28***, ***UBE2M***, ***ZNF42***
RP11-598E05[b]	19p13.2	8.69	**66 (10/15)**	**50 (5/10)**	***OR2Z1***, ***MBD3L1***
RP11-1143D24[a]	19q12	32.59	33 (5/15)	**60 (6/10)**	*No genes*
CTD-2001O24	19	43.4	26 (4/15)	**66 (6/9)**	***SIPA1L3***, ***DPF1***
RP11-79A22	19q13.3	50.09	6 (1/15)	**60 (6/10)**	*CEAL1*, *BCL3*, *CBLC*, *LU*, *PVRL2*, ***TOMM40***, *APOE*, *APOC1*, *APOC4*, *APOC2*, *CLPTM1*, *RELB*, *SFRS16* , *ZNF342*, *GEMIN7*, *XTP7*, *MARK4*, *CKM*, *KLC2L*, *ERCC2*, *PPP1R13L*, *ASE-1*, *ERCC1*, *FOSB*

Genes residing between the two flanking clones of losses are in italics, and with bolded characters for those mapping within clones. Gray-shaded rows indicate clones of the chromosome 19 full-coverage array. Chromosome 7 clones are not included in Table 5 as most GBM cell lines gained the entire chromosome with values fitting $\log_2$ ratio >0.3. [a]High-frequency gained clones with both $\log_2$ ratio >0.5 and >0.3. [b]Clones/genes identified as polymorphic loci in the Genome variation Database (http://projects.tcag.ca.variation). [c]Clones falling in SRO (Table 1).

Discussion

This study reports on an application of high-resolution aCGH to a consistent panel of well-characterized primary glioma cell lines, by means of a 3.5k whole genome plus full-coverage chromosome 19 BAC array. Aiming at the identification of recurrent genomic aberrations involved in glioma genesis and/or progres-

sion towards the highest malignancy grade (WHO grade IV), we systematically compared copy number changes in GBM (WHO grade IV) versus non-GBM cell lines, which included low-grade gliomas (WHO grade I and II) and anaplastic gliomas (WHO grade III). In this context, we took two different and complementary interpretative approaches. The first one is based on single clone frequency analysis, and aims at the definition of the smallest consistently affected intervals of copy number changes. In addition, in order to define clustered clones in consecutive areas of chromosomal imbalance, data analyses was aided by the use of a second, extensive statistical approach known as 'MA approach' (Schraders *et al*., 2005). This approach is considered an important tool to unmask single-copy changes which $\log_2$ ratio values might be underscored particularly in tumors, like gliomas, characterized by high cellular and genetic heterogeneity and ploidy aberrations (Noble and Dietrich, 2004).

In large-scale studies of tumors such as gliomas, for which primary material is hardly ever available for other than diagnostic purposes, primary cell lines have always been considered a good model while studying gliomagenesis (Fischer *et al*., 1985; Bigner *et al*., 1987; Rey *et al*., 1989; Bakir *et al*., 1998). Even with the advent of high-resolution techniques, such as aCGH, a remarkable concordance of findings has repeatedly been demonstrated, with only minute differences, between early passage glioma cell lines and corresponding original tumors (Cowell *et al*., 2004b). Also, the aCGH data on glioma cell lines presented here confirm the known gross aberrations detected on glioma samples by conventional CGH and LOH analyses, such as $+7$, -10 and -22q, thereby further supporting the reliability of cell lines as research tools in cancer genetics of gliomas.

aCGH data processed by the MA approach facilitated the identification of small genomic regions of copy number changes, all representing novel findings in gliomas, with the exception of the gained region detected in GBMs at 1q32.1, which indeed represents a well-known amplification target in malignant gliomas (Riemenschneider *et al*., 2003). Of particular interest because of their specificity to one of our two glioma groups are losses detected in GBMs at 4p16.1, and in non-GBMs at 3p26.1–p26.3, 4q13.2–q21.1 and 7p15.3–p21.1. In particular, losses mapping at the 3p26.1–p26.3 SRO were shared by 8/15 non-GBM cell lines, and were never observed in GBM cell lines. A correlation between 3p losses and low-grade gliomas has been observed in the past in studies focusing on 3p LOH demonstrating that 40% low-grade gliomas showed 3p LOH, while retention of 3p heterozygosity correlated with high pathological grade: accordingly, patients with 3p LOH had a significantly longer survival time than those without LOH (Kanno *et al*., 1997).

In contrast, the remaining SROs we detected at 4p15.31–p15.32, 5q22.2–q23.3, 6p23–p25.3, 11p11.2–q13.2 and 12p13.1–p13.2 are shared by GBMs and non-GBMs, even though some appear to prevail in one of the two groups. Particularly, we observed high deletion frequencies for an SRO mapping to 12p13.1–p13.2, which was found to be lost in three non-GBMs and five GBMs. Single clone analyses also pointed out the involvement of three clones contained in the 12p SRO in at least six GBM lines (60%). 12p has previously been described as site of gain events in gliomas (Weber *et al*., 1996), with amplifications targeting the *CCND2* gene at 12p13.32 (Buschges *et al*., 1999). Our results do not confirm gain/amplification of this locus, but are consistent with the mapping within the 12p SRO of a 12p tumor suppressor locus that has been postulated to be involved in a wide range of hematological malignancies and solid tumors (Montpetit *et al*., 2002).

The 11p11.2–q13.2 SRO gained region is observed in three non-GBMs and three GBMs. The RP11-39G12 clone residing within this SRO shows a high gain frequency in non-GBMs and GBMs (both 50%). Several interesting genes map in the affected interval. Among these, the neurite growth-promoting factor *MDK* has very recently been found amplified in a GBM specimen by aCGH analysis (Cowell *et al*., 2004b). *DDB2*, a DNA repair protein, is involved in the crossresistance of cisplatin-selected cell lines to death ligand-mediated apoptosis (TNF-alpha and Fas-inducing antibody). It functions as a negative regulator of apoptosis because overexpression of *DDB2* suppresses TNF signaling-mediated apoptosis (Sun and Chao, 2005). Therefore, *DDB2* may have a pivotal role in regulating efficacy of anticancer drugs like TRAIL (TNF-related apoptosis-inducing ligand), a promising death ligand for glioma treatment (Hawkins, 2004).

Also the *IG20* gene, which appears to have at least seven splice variants, encodes for a protein involved in the TNF-alpha signaling pathway; overexpression of its isoform DENN-SV, the only one expressed in normal brain, enhances cell replication and resistance to TNF-alpha, vinblastine, etoposide and γ-radiation, supporting the antiapoptotic and cell survival role of DENN-SV (Efimova *et al*., 2004).

In addition, aCGH in combination with the MA approach enabled us to further refine known loci involved in glioma progression, such as, for instance, those on chromosome 10. In GBM, loss of chromosome 10 is the most frequently reported genetic event, commonly accounted for by the presence of tumor suppressors on both 10p and 10q. On 10p, the most frequent site of LOH involves band 10p15 (Harada *et al*., 2000), whereas for the q arm, known or putative tumor suppressor genes as *PTEN* (10q23), *LGI1* (10q24) and *DMBT1* (10q26) are affected in only 30% or less of GBMs, suggesting the presence of additional tumor suppressors genes. More particularly, the 10q25–26 region has been referred to as a target of allelic loss in the majority of GBMs and the *WRD11* gene (10q26) has been proposed as a prime positional candidate gene (Chernova *et al*., 2001).

The 'MA' data analysis of our GBM cell line panel confirmed both the above-mentioned 'hotspots' on chromosome 10 as deletion targets and pointed out three main peaks of most extreme values at 10p15.3, 10q22.3 and 10q26.13–q26.2. The evidence that these peaks do not include the most known candidate genes

led us to assume that other tumor suppressor genes with a critical role in the context of glioma progression might reside within these identified intervals. Interestingly, only the *ADARB2* gene, a brain specific deaminase, resides within the 10p15.3 interval. The *BBCIP* (10q26.6) gene maps within the 10q26.13–q26.2 peak and is among the genes in the interval encompassed by clone RP11-32H11, which is homozygously deleted in the MI-63 cell line. This gene encodes a protein interacting with *BRCA2* and *CDKN1A* (*p21*), which participates in DNA repair and cell cycle control. It has been shown that the BBCIP beta form inhibits cell cycle progression from G1 to S (Meng *et al*., 2004), while its alpha form inhibits brain cancer cell growth, confirming a role as candidate tumor suppressor in brain tumors (Liu *et al*., 2001) as well as in other tumor types (Meng *et al*., 2003).

With regard to chromosome 19, which was interrogated with a full-coverage/tiling path resolution array, one out of the six gliomas with oligodendroglial components and none of the 19 astrocytomas showed deletions at 19q13.3, the well-known LOH area in gliomas, lacking so far any identified tumor suppressor gene (Hartmann *et al*., 2002). It has been recently demonstrated by aCGH that 19q LOH in oligodendrogliomas and mixed OA is due to physical loss of genetic material rather than to genetic events as mitotic recombination (Cowell *et al*., 2004a; Kitange *et al*., 2005). Our data raise the question whether or not in astrocytic tumors 19q LOH involves the same region and is caused by the same mechanisms as in tumors containing oligodendroglial components.

We previously reported that the novel serine threonine kinase *MARK4* gene at 19q13.32 is duplicated in three GBM cell lines, which were also present in the panel used for this study (MI-4, GBM and MI-7) (Beghini *et al*., 2003). By means of the MA algorithm, we found that *MARK4* resides within the region of gain in three non-GBMs and in the GBM cell line MI-4. On the contrary, no gains were detected for cell lines GBM and MI-7.

However, the duplication of *MARK4* we previously described by FISH analysis was characterized through the use of a much smaller contig containing 10 cosmids, of which LLNL-R31237, only containing *MARK4* gene, turned out to be duplicated (Beghini *et al*., 2003). On the other hand, the tiling BAC clones array covering entirely *MARK4* gene span a region containing genes other than *MARK4*. As only the minimal *MARK4* region is duplicated, this would indeed translate into a small fraction of the BAC clones being gained, leading to a very subtle increase in signal intensity. Consequently, we presume that the lack of detection of *MARK4* duplication by aCGH in the above cell lines might be due to the different genomic content of the probes used in these analyses. Interestingly, the MA data analysis highlighted two main gained regions, never before described in gliomas, and mapping to 19p13.11 and 19q13.13–13.2; however, currently no known oncogene has been identified in either one of these two intervals.

Single clone analysis facilitated the identification of very subtle regions not included in the SROs, which, due to their small size, could be directly translated into a limited number of corresponding, and possibly causative genes. Some of these, manifesting as homozygous deletions and found only in GBM cell lines point at tumor suppressor genes including *PTEN* (10q23), *p16* (9p21.3) and *ING1* (13q34) (Zhu and Parada, 2002; Collins, 2004; Tallen *et al*., 2004), which have previously associated with glioma progression. Others are known as putative tumor suppressor genes involved in other cancer types. For instance, *LRP1b* (2q22.3) has been postulated to play an important role in the tumorigenesis of lung cancer (Liu *et al*., 2000), but is expressed predominantly in the brain (Marschang *et al*., 2004). The fact that we reidentified some of these widely acknowledged causative genes in our opinion once more confirms the validity of our approach.

Interestingly, *PRDM2*, a tumor suppressor gene highly expressed in brain tumors (Muraosa *et al*., 1996), represents one of the two genes within the interval of the clone RP11-178M15 at 1p36.21, exclusively lost in 35% of non-GBMs.

Three GBMs showed amplifications at 3q26.3 potentially involving the epithelial-transforming factor (*ECT2*) proto-oncogene, for which an involvement in brain tumors has never been suggested before.

In our cell lines, we did not detect amplification of the *EGFR* gene at 7p11.2, which is found in approximately 40% of primary, but rarely in secondary GBMs (Zhu and Parada, 2002; Collins, 2004). The lack of this finding could be related to the low number in our panel of primary GBMs with an overt *de novo* diagnosis (five of 10 GBMs), and/or to culture conditions, in line with published data suggesting a selection for amplified *EGFR in vivo* and a selection against *EGFR* amplification *in vitro* (Pandita *et al*., 2004) also in early passage cultures (Cowell *et al*., 2004b).

Further validation focusing on the above-mentioned data will be a necessary step to strengthen the candidate regions and genes within or nearby the clones sorted out from our study, and future research might clarify their potential functional role in glioma genesis and/or progression.

The overall achieved insights and their implications increase our current knowledge about subtle genetic changes in gliomas and may facilitate further identification of novel genetic elements, which are of importance in the onset and/or progression of glial tumors. Definition of the multiplicity of genetic elements involved in gliomagenesis provides us with the necessary background needed for the design of novel molecular tools that can be used for an improved diagnostics/therapeutic decision-making in gliomas.

Material and methods

Glioma cell lines

Primary cell lines used for this study included one pilocytic astrocytoma (WHO grade I), five astrocytomas of grade II

including three mixed OAs, nine anaplastic astrocytomas (WHO grade III) including three mixed AOAs, all classified by us as 'non-GBMs', and 10 gliomas of grade IV (GBMs). Within grade IV, four *de novo* (primary) GBMs, one secondary (arisen from a previous astrocytoma) GBM, three apparently secondary GBMs (based on tumoral differentiated areas within the specimen, but not attested by previous surgery or anamnesis), one primary giant cell and one apparently secondary giant cell GBM are included.

Primary glioma cell lines were established from biopsy fragments using methods described previously (Magnani *et al*., 1994). The GBM (Perego *et al*., 1994) and MI-4 (Magnani *et al*., 1994, 1999, 2005) cell lines were used at 33rd and 61st passage, respectively, whereas all other cell lines were used before their 14th passage. All cell lines were maintained in RPMI 1640 medium containing 5% FCS at 37°C and 5% CO_2.

WHO classification, clinical data and cytogenetic analysis of the fresh tumors of origin, when available, are provided in Supplementary Table A. All karyotypes were described according to *ISCN 95* guidelines (Mitelman, 1995).

Additional karyotyping was performed on MI-4, MI-60 (Magnani *et al*., 1999), GBM and MI-7 (Magnani *et al*., 1999) cell lines at the first passages. The first three cell lines presented the same stemline karyotype described primarily, whereas the karyotype of MI-7 revealed a subclone containing 59 chromosomes in addition to the original tumor (46, X, −Y, +7/59, XY, +1, +del(3q) × 2, −4, +5, +6, +7, +7, +7, add9q34, −12, −13, +16, +19, +20, +21, +21, +1).

Array-based CGH

aCGH hybridizations were performed on microarrays containing approximately 4300 BAC clones. These BAC clones can be subdivided in approx. 3600 BAC clones that are equally distributed over the entire human genome with an average 800 kb resolution (Schraders *et al*., 2005) and approx. 700 BAC clones that cover close to the entire chomosome 19 at tiling path resolution. For chromosome 19, a full-coverage set containing approc. 700 chromosome-specific, finger-printed and phage-tested BAC clones was selected from a larger '32k set', which was developed at the British Columbia Cancer Agency Genome Sciences Center, Vancouver, Canada (Krzywinski *et al*., 2004). This subset covers chromosome 19 with an average resolution of 100 kb. Preparation of BAC arrays, labeling and hybridizations were performed essentially as described by Vissers *et al*. (2003). All hybridizations were performed on the same batch of quality controlled arrays, thereby excluding minor batch-to-batch differences.

Analysis of the microarray images obtained from the BAC hybridizations was performed using the software package GenePix Pro 4.0 (Axon Instruments Inc., Foster City, CA, USA). For each spot, the median pixel intensity minus the median local background for both dyes was used to obtain a genomic copy number ratio. Data normalization was performed in the software package SAS version 8.0 (SAS Institute Inc.) for each array subgrid, by applying Lowess curve fitting with a smoothing factor of 0.3 to predict the $\log_2$-transformed test-over-reference (T/R) value on the basis of the average logarithmic fluorescent intensities (Cleveland, 1979). All mapping information regarding clone locations, cytogenetic assignments and gene content were retrieved from the UCSC human genome browser (http://genome.ucsc.edu/, May 2004 freeze).

Statistical analysis

To detect areas of nonoverlapping gained and lost consecutive clones, we applied an algorithm that we have recently described (Schraders *et al*., 2005) based on extreme values of MAs of normalized $\log_2$ ratios with different window sizes. Mathematical/statistical details underlying this algorithm are available upon request (H.straatman@epib.kun.nl). The most extreme MA in all cell lines was above +0.1 or below −0.1, with the exception of two areas, one at 3p and the other at 7p (the most centromeric) (Figure 1), both with a mean of −0.09 with a window width of 24 and 27 clones, respectively. The MA algorithm was used in six normal versus normal hybridizations to identify false-positive areas caused by underperformance of individual clones or novel polymorphic regions/large-scale copy number variations (LCVs). All areas of copy number changes identified in cell line samples by MAs with a window width from 2 to 10 were excluded even if present only once in normal versus normal hybridizations, and the same approach was adopted for MAs with a window width from 11 to 30. The only exception was one deleted interval at 4p, where in normal versus normal hybridizations three extreme MAs were detected: the first, with a mean of −0.22 and a window width of eight clones in cell line samples showed higher mean values ranging from −0.35 to −0.57. The other two extreme MAs, with a window width from 11 to 30, showed a mean of −0.14 and −0.17 in normal versus normal hybridizations. Therefore, we included in the analysis only MAs with a window width from 11 to 30 below −0.3 in cell line samples.

For whole chromosome association analysis, a chromosome was scored as gained or lost when: (a) 90% of all clones on the chromosome had a $\log_2$ ratio $>$ or <0, respectively; (b) the median of the $\log_2$ ratio of all clones on that chromosome was $>$ or <0.1 or -0.1, respectively (Hackett *et al*., 2003). Samples were hybridized in sex-mismatch hybridization schemes, allowing for a quick objective general assessment of the quality of individual experiments by determination of average normalized T/R values for the sex chromosomes. For this reason, sex chromosomes were excluded for further analysis.

Single clone analysis

As a first step, 'suspicious clones', which were defined as clones that have either a standard deviation >0.26 or <0.026 or a z-value (average ratio/standard error) >5 in the normal versus normal hybridizations (references), were discarded. In addition, clones showing a standard deviation $d>0.3$ over triplicate in the individual experiments were excluded, as well as clones with less than two replicates remaining after this analysis.

Subsequently, copy number changes were scored as gains or losses when the normalized mean $\log_2$ (test/reference) ratio was $>+0.3$ or <-0.3, respectively. These boundaries were arbitrarily set by examining the results of the normal versus normal hybridizations and supported by the results of previously published work (Veltman *et al*., 2003a, b; Vissers *et al*., 2003). To detect hotspots of genomic imbalances, we excluded from the analysis clones showing copy number changes in one or more of the six normal versus normal hybridizations. We subsequently established a 'threshold of significance', including in the analysis only informative clones in at least 5/6 normal versus normal, 10/15 'non-GBMs' versus normal and 7/10 'GBMs' versus normal hybridizations. Clones of interest were selected on the basis of the highest frequencies of aberration calculated on informative clones in either 'non-GBM' or GBM specimens.

All information regarding physical maps and genomic content of clones was obtained through the UCSC human genome browser (http://genome.ucsc.edu/, May 2004 freeze), and clones were queried as possible LCVs or CNPs (copy number polymorphisms) at the Genome Variation Database

(http://projects.tcag.ca.variation) (Iafrate *et al*., 2004; Sebat *et al*., 2004).

Acknowledgements

This work was supported by AIRC (Associazione Italiana Ricerca sul Cancro) 2003 grant (to LL) and a Dutch Cancer Society grant (KWF-KUN 2004-3143) to a local research consortium including ES. We acknowledge the EC COST support through the COST ACTION B19 'Molecular cytogenetics of solid tumors' short-term scientific mission (to GR) and collaboration thereafter primed in carrying out this work. We acknowledge Prof M Rocchi for providing us several BAC clones useful for FISH analyses.

References

Bakir A, Gezen F, Yildiz O, Ayhan A, Kahraman S, Kruse CA *et al*. (1998). *Cancer Genet Cytogenet* **103**: 46–51.
Beghini A, Magnani I, Roversi G, Piepoli T, Di Terlizzi S, Moroni RF *et al*. (2003). *Oncogene* **22**: 2581–2591.
Bigner SH, Mark J, Bigner DD. (1987). *Cancer Genet Cytogenet* **24**: 163–176.
Bredel M, Bredel C, Juric D, Harsh GR, Vogel H, Recht LD *et al*. (2005). *Cancer Res* **10**: 4088–4096.
Buschges R, Weber RG, Actor B, Lichter P, Collins VP, Reifenberger G. (1999). *Brain Pathol* **9**: 435–442.
Cairncross JG, Ueki K, Zlatescu MC, Lisle DK, Finkelstein DM, Hammond RR *et al*. (1998). *J Natl Cancer Inst* **90**: 1473–1479.
Chernova OB, Hunyadi A, Malaj E, Pan H, Crooks C, Roe B *et al*. (2001). *Oncogene* **20**: 5378–5392.
Cleveland WS. (1979). *J Am Stat Assoc* **74**: 829–836.
Collins VP. (2004). *J Neurol Neurosurg Psychiatry* **75**(Suppl 2): ii2–ii11.
Cowell JK, Barnett GH, Nowak NJ. (2004a). *J Neuropathol Exp Neurol* **63**: 151–158.
Cowell JK, Matsui S, Wang YD, LaDuca J, Conroy J, McQuaid D *et al*. (2004b). *Cancer Genet Cytogenet* **151**: 36–51.
Efimova EV, Al-Zoubi AM, Martinez O, Kaithamana S, Lu S, Arima T *et al*. (2004). *Oncogene* **23**: 1076–1087.
Fischer H, Schwechheimer K, Heider M, Bernhardt S, Zang KD. (1985). *Cancer Genet Cytogenet* **17**: 257–268.
Hackett CS, Hodgson JG, Law ME, Fridlyand J, Osoegawa K, de Jong PJ *et al*. (2003). *Cancer Res* **63**: 5266–5273.
Harada K, Nishizaki T, Maekawa K, Kubota H, Harada K, Suzuki M *et al*. (2000). *Genomics* **67**: 268–272.
Hartmann C, Johnk L, Kitange G, Wu Y, Ashworth LK, Jenkins RB, *et al*., Transcript Map of the 3.7-Mb D19S112–D19S246. (2002). *Cancer Res* **62**: 4100–4108.
Hawkins CJ. (2004). *Vitam Horm* **67**: 427–452.
Iafrate AJ, Feuk L, Rivera MN, Listewnik ML, Donahoe PK, Qi Y *et al*. (2004). *Nat Genet* **36**: 949–951.
Ino Y, Betensky RA, Zlatescu MC, Sasaki H, Macdonald DR, Stemmer-Rachamimov AO *et al*. (2001). *Clin Cancer Res* **7**: 839–845.
Jeuken JW, von Deimling A, Wesseling P. (2004). *J Neurooncol* **70**: 161–181.
Kanno H, Shuin T, Kondo K, Yamamoto I, Ito S, Shinonaga M *et al*. (1997). *Cancer Res* **57**: 1035–1038.
Kitange G, Misra A, Law M, Passe S, Kollmeyer TM, Maurer M *et al*. (2005). *Genes Chromosomes Cancer* **42**: 68–77.
Kitange GJ, Templeton KL, Jenkins RB. (2003). *Curr Opin Oncol* **15**: 197–203.
Kleihues P, Cavenee WK. (2000). *Pathology and Genetics of Tumours of the Nervous System*. IARC Press: Lyon, pp. 99–102.
Kohler B, Wolter M, Blaschke B, Reifenberger G. (2004). *Int J Cancer* **111**: 644–645.
Koschny R, Koschny T, Froster UG, Krupp W, Zuber MA. (2002). *Cancer Genet Cytogenet* **135**: 147–159.
Krzywinski M, Bosdet I, Smailus D, Chiu R, Mathewson C, Wye N *et al*. (2004). *Nucleic Acids Res* **32**: 3651–3660.
Liu CX, Musco S, Lisitsina NM, Forgacs E, Minna JD, Lisitsyn NA. (2000). *Cancer Res* **60**: 1961–1967.
Liu J, Yuan Y, Huan J, Shen Z. (2001). *Oncogene* **20**: 336–345.
Magnani I, Chiariello E, Conti AM, Finocchiaro G. (1999). *Cancer Genet Cytogenet* **110**: 82–86.
Magnani I, Guerneri S, Pollo B, Cirenei N, Colombo BM, Broggi G *et al*. (1994). *Cancer Genet Cytogenet* **75**: 77–89.
Magnani I, Moroni RF, Roversi G, Beghini A, Pfundt R, Schoenmakers EFPM *et al*. (2005). *Cancer Genet Cytogenet* **161**: 140–145.
Manni I, Tunici P, Cirenei N, Albarosa R, Colombo BM, Roz L *et al*. (2002). *Br J Cancer* **86**: 477–484.
Marschang P, Brich J, Weeber EJ, Sweatt JD, Shelton JM, Richardson JA *et al*. (2004). *Mol Cell Biol* **24**: 3782–3793.
Meng X, Liu J, Shen Z. (2003). *Gene* **302**: 139–146.
Meng X, Liu J, Shen Z. (2004). *Cell Cycle* **3**: 343–348.
Mischel PS, Cloughesy TF, Nelson SF. (2004). *Nat Rev Neurosci* **5**: 782–792.
Mitelman F. (Ed). (1995). *LSCN (1995): An International System for Human Cytogenetic Nomenclature*. S. Karger: Basel.
Montpetit A, Boily G, Sinnett D. (2002). *Eur J Hum Genet* **10**: 62–71.
Muraosa Y, Takahashi K, Yoshizawa M, Shibahara S. (1996). *Eur J Biochem* **235**: 471–479.
Nigro JM, Misra A, Zhang L, Smirnov I, Colman H, Griffin C *et al*. (2005). *Cancer Res* **65**: 1678–1686.
Noble M, Dietrich J. (2004). *Trends Neurosci* **27**: 148–154.
Ohgaki H, Schauble B, zur Hausen A, von Ammon K, Kleihues P. (1995). *Virchows Arch* **427**: 113–118.
Pandita A, Aldape KD, Zadeh G, Guha A, James CD. (2004). *Genes Chromosomes Cancer* **39**: 29–36.
Perego P, Boiardi A, Carenini N, De Cesare M, Dolfini E, Giardini R *et al*. (1994). *J Cancer Res Clin Oncol* **120**: 585–592.
Rey JA, Bello MJ, de Campos JM, Kusak ME, Moreno S. (1989). *Cancer Genet Cytogenet* **41**: 175–183.
Riemenschneider MJ, Knobbe CB, Reifenberger G. (2003). *Int J Cancer* **104**: 752–757.
Ritland SR, Ganju V, Jenkins RB. (1995). *Genes Chromosomes Cancer* **12**: 277–282.
Rong Y, Post DE, Pieper RO, Durden DL, Van Meir EG, Brat DJ. (2005). *Cancer Res* **65**: 1406–1413.
Schmidt MC, Antweiler S, Urban N, Mueller W, Kuklik A, Meyer-Puttlitz B *et al*. (2002). *J Neuropathol Exp Neurol* **61**: 321–328.
Schraders M, Pfundt R, Straatman HM, Janssen IM, van Kessel AG, Schoenmakers EF *et al*. (2005). *Blood* **105**: 1686–1693.
Sebat J, Lakshmi B, Troge J, Alexander J, Young J, Lundin P *et al*. (2004). *Science* **305**: 525–528.

Shapiro J R. (2002). *Am J Med Genet* **115**: 194–201.
Simpson JR, Horton J, Scott C, Curran WJ, Rubin P, Fischbach J *et al*. (1993). *Int J Radiat Oncol Biol Phys* **26**: 239–244.
Smith JS, Alderete B, Minn Y, Borell TJ, Perry A, Mohapatra G *et al*. (1999). *Oncogene* **18**: 4144–4152.
Sun CL, Chao CC. (2005). *Mol Pharmacol* **67**: 1307–1314.
Tallen G, Kaiser I, Krabbe S, Lass U, Hartmann C, Henze G *et al*. (2004). *Int J Cancer* **109**: 476–479.
Veltman JA, Jonkers Y, Nuijten I, Janssen I, van der Vliet W, Huys E *et al*. (2003a). *Am J Hum Genet* **72**: 1578–1584.
Veltman JA, Fridlyand J, Pejavar S, Olshen AB, Korkola JE, DeVries S *et al*. (2003b). *Cancer Res* **63**: 2872–2880.
Vissers LE, de Vries BB, Osoegawa K, Janssen IM, Feuth T, Choy CO *et al*. (2003). *Am J Hum Genet* **73**: 1261–1270.
von Deimling A, Bender B, Jahnke R, Waha A, Kraus J, Albrecht S *et al*. (1994). *Cancer Res* **54**: 1397–1401.
von Deimling A, Louis DN, von Ammon K, Petersen I, Wiestler OD, Seizinger BR. (1992). *Cancer Res* **52**: 4277–4279.
Weber RG, Sabel M, Reifenberger J, Sommer C, Oberstrass J, Reifenberger G *et al*. (1996). *Oncogene* **13**: 983–994.
Zhu Y, Parada LF. (2002). *Nat Rev Cancer* **2**: 616–626.

Supplementary Information accompanies the paper on Oncogene website (http://www.nature.com/onc)